Low-level nutrient enrichment during thermal stress delays bleaching and ameliorates calcification in three Hawaiian reef coral species

Ji Hoon J. Han[1], Matthew P. Stefanak[1*], and Ku'ulei S. Rodgers[1]

[1]Hawai'i Institute of Marine Biology, University of Hawai'i at Mānoa, 46-007 Lilipuna Rd. Kāne'ohe, HI 96744, USA

Corresponding Author:
Ji Hoon J. Han[1]
46-007 Lilipuna Road Kāne'ohe, HI 96744, USA
Email address: han9@hawaii.edu

*Current Address
University of Maryland, Center for Environmental Science
Chesapeake Biological Laboratory
146 Williams St.
Solomons, MD 20688

Introduction

Coral reef systems are threatened globally by the pernicious effects of sea surface temperature (SST) rise, which can expose the coral holobiont to considerable thermal stress and potentially lead to mass bleaching events (Hughes et al. 2017). Coral bleaching, the process of major expulsion or digestion of zooxanthellae from or by the host, is instigated by the breakdown of the mutualistic relationship between coral and endosymbiont. These symbionts, along with host pigments in some species, give coral their characteristic coloration. The diminishment of color during bleaching thus results from the loss of these symbionts, which often then reveals the white skeleton beneath the now transparent tissues. Although the primary cause of widespread bleaching is considered to be heat stress (Hoegh-Guldberg et al. 2007), other large-scale chronic and acute factors exist that can induce and exacerbate reef-wide bleaching, including ocean acidification (Andersson et al. 2009; Jokiel et al. 2013) and shifts in salinity, sedimentation, or irradiance (Easterling 2000; Rodgers et al. 2021). Although repopulation by symbionts is possible under brief temperature deviations, sustained bleaching can lead to whole colony mortality (Jokiel & Coles 1990). Given many coral species live within only 1-2 °C of their upper thermal limits (Coles et al. 1976; Jokiel & Coles 1977), observed increases in mean decadal SSTs are particularly harrowing given predictions of continual elevations in temperature due to climate change. If global mean surface temperature increases reach 1.5-2.0 °C above pre-industrial levels, warm-water reef mortality is expected to reach 70-90% worldwide (Hoegh-Guldberg et al. 2019).

The physiological mechanisms that drive coral bleaching have largely focused on photo-oxidative stress via photoinhibition of endosymbionts (Iglesias-Prieto et al. 1992; Lesser 2006; Weis 2008). The buildup of excess heat energy is partially transferred to oxygen, increasing concentrations of reactive oxygen species (ROS), which can cause substantial zooxanthellate cellular damage (Smith et al. 2005; Weis 2008), followed by the release of ROS into host cells (Downs et al. 2002) and eventual apoptosis (Dunn et al. 2004). More recent studies, however, have

46 posited that amplified ROS-associated toxicity is at least preceded by independent host-specific
47 immune responses to thermal stress (Krueger et al. 2015). Rädecker et al. (2021) found that
48 temperature-associated increases in host energy demand may spur shifts in metabolism to reliance
49 on amino acid catabolism, resulting in ammonium release and subsequent uptake by
50 endosymbionts. This catalyzes algal growth, leading to decreased translocation of photosynthate
51 to host cells and, ultimately, the degradation of symbiosis. These findings are particularly notable
52 given that host mortality is thought to be driven at least in part by coral starvation (Anthony et al.
53 2007).
54   Many local scale environmental factors also exist that can induce coral bleaching and
55 mortality. Excess terrestrial nutrient input, which is commonly introduced through anthropogenic
56 point sources (e.g., drain and sewage pipes) and non-point sources (e.g., impervious surface runoff,
57 landslides), has been increasing due to shoreline development, agricultural activity, and storm
58 frequency and intensity (Carlson et al. 2019; Giambelluca et al. 2013). Dissolved inorganic
59 nutrients, such as phosphate (PO_4^{-3}), nitrate + nitrite (NO_2^- + NO_3^-), and ammonium (NH_4^+), are
60 essential components in marine ecosystem functioning that govern biological productivity in
61 marine environments (Smith 1984). Most warm-water corals have evolved in nutrient-limited
62 oligotrophic habitats, thus even minor augmentations of nutrient concentrations can lead to a
63 variety of direct and indirect effects on coral health and metabolism.
64   Coral responses to nutrient elevation are differential, varying by species, local nutrient
65 history, and nutrient type, concentration, and ratio (Bongiorni et al. 2003; Burkepile et al. 2020;
66 Fabricius 2005; Fox et al. 2021; Tanaka et al. 2017). A meta-analysis of historical nutrient research
67 described how nitrogen enrichment oftentimes reduced calcification and enhanced photosynthesis
68 in corals while, in contrast, phosphorous enrichment increased calcification with minimal effects
69 on coral photosynthesis (Shantz and Burkepile 2014). The role of nutrients in complex external
70 and internal processes of coral holobiont metabolism, however, is not well understood.
71   Ammonium is the preferred source of dissolved inorganic nitrogen (DIN) for corals over
72 nitrate and nitrite (Grover et al. 2003; Grover et al. 2008), which require reduction to be available
73 for myriad metabolic processes. Several seminal laboratory studies have shown that exposure to
74 relatively moderate concentrations of DIN (>2 µM) is associated with increased zooxanthellae
75 density, chlorophyll concentration, and/or gross photosynthesis (Ezzat et al. 2019; Ferrier-Pages
76 et al. 2000; Marubini & Davies 1996; Muscatine et al. 1998; Stambler et al. 1991). These
77 responses, however, are not necessarily indicative of healthy symbioses (i.e., reduced carbon
78 translocation from higher endosymbiont population, see Dubinsky & Jokiel (1994)) and are
79 inconsistent across different studies (perhaps due to variable experimental design), while
80 oftentimes also accompanied by evidence of lowered calcification rates at higher concentrations
81 (5-20 µM) of DIN (Fabricius 2005). Moreover, it has been shown that dissolved inorganic
82 phosphorous (DIP) exposure, although leading to higher growth rates, reduced skeletal density in
83 new growth and thus affected structural quality (Dunn et al. 2012). More recent studies have found
84 that, in the absence of concurrent DIP increases, sustained elevation of DIN concentrations may
85 lead to phosphorous starvation and subsequent reduction in photosynthetic efficiency and carbon
86 metabolism (D'Angelo & Wiedenmann 2014; Ezzat et al. 2015; Rosset et al. 2017). Studies such
87 as these have led to the development of a nutrient-response paradigm that is principally dependent
88 on the nitrogen to phosphorous (N:P) ratio, which, if insufficiently balanced from DIN over-
89 enrichment, can lead to degradation of the host-endosymbiont mutualism (D'Angelo &
90 Wiedenmann 2014; Morris et al. 2019; Tanaka et al. 2017). These studies, however, only applied
91 nitrate as a DIN enrichment source, which is typically not as preferential as ammonium and

92   generally causes deleterious effects at higher concentrations as compared to ammonium (Ezzat et
93   al. 2015; Marangoni et al. 2020). On a community-wide scale, elevated nutrient input can stimulate
94   excess macroalgal growth (Fabricius 2005), which oftentimes leads to coral mortality via algal
95   stressors such as overgrowth and shading (McCook et al. 2001), inhibition of larval viability and
96   settlement (Kuffner et al. 2006), and (or) allelochemical toxicity (Vieira et al. 2016). In cases of
97   large-scale proliferation, lasting or permanent phase shifts from coral-dominant to algal-dominant
98   regimes can occur, leading to shifts in community species composition and reductions in
99   biodiversity (Adam et al. 2021; Duprey et al. 2016).
100   The combination of elevated anthropogenically-sourced DIN and increased sea surface
101   temperatures has long been considered as negatively synergistic with respect to coral health.
102   Wooldridge & Done (2009) described how excess DIN exposure during thermal stress may
103   preclude zooxanthellae from homeostatic growth-limitation, thus resulting in withholding of
104   endosymbiont carbon translocation to the host during heat stress when it is particularly crucial,
105   thus decreasing bleaching resiliency. Indeed, higher densities of algal symbionts have been shown
106   to escalate susceptibility to bleaching (Cunning & Baker 2013). Empirically, several field studies
107   have linked elevated heat and anthropogenic nitrate to increases in bleaching susceptibility and
108   intensity (Burkepile et al. 2020; Donovan et al. 2020). Furthermore, when considering ratio-
109   dependent nutrient load, Wiedenmann et al. (2013) found that imbalanced increases in nitrate and
110   concomitant phosphate starvation led to both greater susceptibility of bleaching during thermal
111   stress and lowered thermal limits. Similarly, Chumun et al. (2013) observed more damage to
112   endosymbionts under imbalanced high heat and nitrate conditions, in addition to impediment of
113   recovery post-stress. Nitrate elevation-induced phosphate starvation may be especially harmful
114   during heating given the finding that phosphate uptake rate is significantly higher during heat
115   stress, which suggests an important role of DIP in bleaching resiliency during heating (Ezzat et al.
116   2016). While several studies treated nitrate (NO_3^-) as the main DIN source, recent studies have
117   found that differential nitrogen identities (i.e., nitrate, ammonium, and (or) urea) can result in
118   various physiological responses (e.g., Burkepile et al. 2020; Marangoni et al. 2020). Contrasting
119   responses of bleaching intensity under thermal stress have indeed been found, with positive effects
120   under ammonium (NH_4^+) enrichment versus negative effects of nitrate (NO_3^-) enrichments (Ezzat
121   et al. 2019; Marangoni et al. 2020).
122   Despite many cases of decline, there have been some instances suggesting nutrients may
123   have the ability to lessen or delay the effects of thermal stress under balanced ratio conditions
124   (Wiedenmann et al. 2013). To our knowledge, this was first observed by McClanahan et al. (2003),
125   where fertilizer containing high amounts of phosphoric acid, ammonium, and nitrate reduced
126   paling from seasonal bleaching in treated colonies. Since then, Beraud et al. (2013) have found
127   that balanced enrichment with ~3-3.8 µM ammonium during thermal stress resulted in an increased
128   rate of photosynthetic activity and calcification when compared to heat-only treatments. More
129   recently, when comparing the effects of nitrate and ammonium during heating, Marangoni et al.
130   (2020) also recorded beneficial responses to 3 µM of ammonium with a balanced N:P ratio (~17:1)
131   in the form of photosynthetic activity, calcification, and gauges of oxidative damage, although
132   nitrate did not share these outcomes. Lastly, after minor yet chronic (~15 months) artificial
133   increases in nitrate + nitrite, ammonium, and phosphate (on average 0.14 µM, 0.14 µM, and 0.22
134   µM, respectively), Becker et al. (2021) found improved holobiont performance under thermal
135   stress, namely higher rates of maximal photosynthetic performance and oxygen evolution in
136   nutrient-enriched groups. Despite several articles showing the potential of low nutrient enrichment
137   to ameliorate various impacts of thermal stress, the type of enriched nutrients and N:P ratios largely

138 vary by study and thermal stress period and were all restricted to less than one week. Although
139 low enrichment under thermal stress has been shown to cause temporary changes in coral
140 physiology that are beneficial, under longer periods of thermal stress these changes may be
141 detrimental. There have been no published studies that have investigated the long-term effects of
142 low nutrient enrichment under extended chronic thermal stress until this study.
143   To represent the prolonged duration of summer bleaching events in Hawai'i more closely,
144 we exposed three species of Hawaiian reef corals (*Lobactis scutaria*, *Montipora capitata*, and
145 *Pocillopora acuta*) to increases of <1 μM of nitrate + nitrite, ammonium, and phosphate above
146 ambient concentrations for 31 days under high temperature conditions. Of the species evaluated in
147 this study, *Pocillopora acuta* has the lowest temperature threshold, followed by *Montipora*
148 *capitata* (Jokiel & Brown 2004; Ritson-Williams & Gates 2020), while the more cryptic *Lobactis*
149 *scutaria* is more resilient to elevated temperatures (Bahr et al. 2016); species that exhibit higher
150 resistance to bleaching can be characterized by massive growth forms, thicker tissues, and
151 heterotrophic feeding as in the solitary coral *L. scutaria*. Given these species-specific tolerances
152 to heat stress, we expected differential responses to nutrient and (or) thermal stress. This study was
153 undertaken using mesocosm tanks that create conditions comparable to the field yet allow for
154 manipulation of seawater input (Jokiel et al. 2014). Colony samples were collected from Kāne'ohe
155 Bay, which has a history of nutrient pollution, although substantial reductions in anthropogenic
156 inputs have occurred following the relocation of sewage effluent offshore in 1979 (Smith et al.
157 1981). The high nutrient, anoxic, and low light conditions prior to sewage removal led to an
158 extreme decrease in coral cover and a simultaneous increase in filter or deposit feeders,
159 phytoplankton, and algae (Hunter & Evans 1995; Laws & Redalje 1982). This historical exposure
160 to nutrient stress may have increased resilience to nutrient elevation in resident corals. Recent
161 research has also shown that corals in Kāne'ohe Bay are more acclimatized to thermal stress (Coles
162 et al. 2018; Jury & Toonen 2019) and may likewise be more resilient to nutrient stress. Response
163 variables measured by visual assessment included partial and full colony bleaching and mortality.
164 Calcification rates were quantified using the buoyant weighing technique and compared before
165 and after heat exposure. Given outcomes from previously described studies, we expected that
166 nutrient-enriched groups under thermal stress would show smaller decreases in calcification rate
167 and reduced prevalence of bleaching and mortality during or at the end of the heating period.
168
169 **Materials & Methods**
170 *Experimental Design*
171   The study period in this experiment spanned from June 21st to August 12th of 2019. A total
172 of 360 coral colonies were collected, comprised of 120 individuals from three local species:
173 *Lobactis scutaria* (Ls), *Montipora capitata* (Mc), and *Pocillopora acuta* (Pa).
174   All coral collections were authorized under a Division of Aquatic Resources Special
175 Activities Permit SAP 2019-16. The reference to *Pocillopora* colonies as *P. acuta*, as opposed to
176 their ostensible historical identification as *P. damicornis*, was implemented based on recent
177 findings that *P. acuta* are commonly misidentified as *P. damicornis* in our study site of Kāne'ohe
178 Bay (Johnston et al. 2018). Colonies from each species were separated into four distinctive thermal
179 and nutrient groups (Fig. 1), hereafter referred to by their abbreviations: a control group of ambient
180 heat and nutrient levels ("A"), an ambient heat and elevated nutrient group ("N"), an elevated heat
181 and ambient nutrient group ("H"), and an elevated heat and nutrient group ("NH"). As such, this
182 led to a nested study design with mesocosm tank nested within treatment group and species. Target

183 temperature increases in heat-treated groups were set at 31 °C. Ambient temperature and nutrient
184 levels were representative of Kāne'ohe Bay field conditions due to direct seawater influx.
185   The study period was separated into consecutive acclimation and heating phases (Fig. 2).
186 The initial acclimation phase lasted for 22 days (21 June – 12 July 2019) with the intention of
187 acclimating corals to mesocosms and, for nutrient-treated colonies, elevated nutrient
188 concentrations. Following the acclimation phase, temperature was raised in heat-treated groups for
189 31 days (13 July – 12 August 2019), which was defined as the heating phase. Nutrient elevation in
190 treated groups was continuous throughout all phases. Measured temperatures and nutrient
191 concentrations during each phase are shown by treatment group in Table 1 and Table 2,
192 respectively.
193
194 *Sample Site & Colony Collection*
195   Kāne'ohe Bay is located in northeast O'ahu, Hawai'i (21° 24' 49.799" N and 157° 47'
196 39.146" W). It is the largest sheltered body of water in the Main Hawaiian Islands (MHI),
197 approximately 28 km^2 in size with a maximum depth of 12 meters. Several reef structures can be
198 found within the embayment. A fringing reef runs along the shoreline with over 50 patch reefs
199 located within the lagoonal waters. The outer reef is composed mainly of limestone with a basalt
200 foundation and is not a true barrier reef but is referred to as one.
201   Colonies of similar size and morphology of the three study species were collected from the
202 Moku o Lo'e shallow reef flat located adjacent to the research site at the Coral Reef Ecology
203 Laboratory on the eastern point of the island (Fig. 3). All samples were collected from a depth of
204 approximately one-half meter with colony size approximately 15 cm and limited to 200 g in
205 weight. Colonies with partial damage or that showed signs of the disease were not collected.
206 Conspecifics were gathered several meters apart to avoid genetic redundancy by fragmentation.
207 Selected colonies were placed on underwater trays for transport and remained submerged during
208 the transfer to laboratory tanks, where they were held for one week in gradually reduced shaded
209 conditions to remediate any transfer-related stress. Following this respite period, ten randomly
210 selected colonies of each species were assigned to each of the twelve 660-liter (1 m x 1 m x 0.5
211 m) fiberglass flow-through mesocosms for a total of 30 colonies per tank (Fig. 1).
212
213 *Mesocosm Flow-Through System*
214   The mesocosm tank system in this study modeled that of tanks originally designed by
215 Jokiel & Coles (1978) in order to closely replicate the environmental conditions (e.g., depth, light
216 level, irradiance, etc.) of the reef flat collection site in Kāne'ohe Bay. To limit fouling, water inflow
217 was alternated through two intake pipes monthly. Additionally, the two separate lines transporting
218 water from the intake pipe to the mesocosm system were reamed and switched monthly. Mesocosm
219 water turnover (flow) rate was determined by closing the tail box drain and recording the time for
220 water outflow to reach 10 L. Turnover rate was measured at least twice per day to ensure that all
221 tanks had rates lower than 55 sec/10 L (< 60 min per complete turnover) to meet previously
222 determined flow rate requirements described by Jokiel et al. (2008). To maintain water circulation,
223 two Marineland® Maxi-Jet® 1200 multi-use water pump and powerheads were placed diagonally
224 in the top corners of all tanks and set at the max rate of 295 gallons/hour. Tank oxygenation was
225 sustained through an aeration stone that was centered at the bottom of the mesocosm. Water quality
226 factors such as salinity, dissolved oxygen, and pH were monitored daily using a YSI-556 Handheld
227 Multiparameter Water Quality Meter, although no anomalous conditions were detected over the
228 course of the study period.

229
230   *Abiotic Factor Manipulation & Measurement*
231   Finnex® TH Deluxe Titanium 800-Watt heating units were placed in all heat-treated
232   mesocosms (NH and H) and were continuously active. Additionally, BlueLine Biotherm Titanium
233   Aquarium 1000-W heaters (Model IPX8) were also employed to reach target temperatures; all
234   1000-W heaters were connected to Aqua Logic, Inc. Single Stage digital temperature controllers
235   (model TR115SN), which activated 1000-W heaters when temperature fell to 30.8º C and
236   deactivated heaters when temperature reached 31 ºC. Heaters were placed in identical locations
237   and orientations within each heat-treated mesocosm. Temperature was also recorded in all
238   mesocosms during the entirety of the study period using calibrated Onset ProV2 HOBO automatic
239   temperature loggers, which collected temperature estimates at 30-min intervals. Mean
240   temperatures in the heated treatments (30.72ºC) (H, NH) were maintained at a level of ~2.2 ºC
241   above non-heated treatment groups during the heating phase (Table 1).
242   Nutrient concentrations in modified treatment groups (N and NH) were elevated by
243   dissolving 39.879 grams of sodium nitrate (NaNO$_3$), 33.465 grams of ammonium chloride
244   (NH$_4$Cl), and 29.799 grams of monopotassium phosphate (KH$_2$PO$_4$) into 100 L of ambient
245   seawater from the adjacent reef flat. This resulted in an N:P ratio enrichment of approximately
246   1.94:1. Altered seawater was stored in a 100-L Nalgene™ cylindrical polypropylene reservoir tank
247   and replenished using the same seawater to nutrient concentration ratios. To transfer nutrient-
248   elevated seawater to selected mesocosms, a Cole-Parmer Masterflex® L/S Digital Drive EW-
249   7523-80 was attached to two Cole-Parmer Masterflex® L/S Multichannel (model 7535-04)
250   peristaltic pumps set at 5 mL/min. The peristaltic pump moved seawater through six 16"
251   Masterflex® Pump Tubings (model 96400-16), which were then connected to six less-flexible
252   black polyethylene drip irrigation tubes (width 1.5cm) that extended to the mesocosms.
253   Nutrient concentrations were measured weekly in each tank for the duration of the study
254   period. Prior to sampling, twelve 1-L opaque Nalgene™ bottles were acid-washed using an 8%
255   acetic acid solution. Bottles were then thrice rinsed with demineralized water and mesocosm water.
256   To rinse, one-third of the bottle was filled then gently rotated and agitated for at least 15 seconds.
257   Following rinsing, 1-L of mesocosm water was collected from same depth as coral colonies. 100
258   mL of sampled water was filtered through a GF/F 25 mm Whatman glass microfiber filter into a
259   125 mL Nalgene™ bottle using a 60 mL syringe. A new filter was used for every water sample.
260   Additionally, from the onset of the heating phase, bimonthly water samples were gathered at
261   approximately 1 m in depth from field sites adjacent to the mesocosm intake pipe and the South
262   Bay location (Fig. 3). Laboratory and field water samples were kept at -20º C until their transport
263   to the University of Hawai'i School of Ocean and Earth Science and Technology Laboratory (S-
264   LAB) for analysis. All nutrient concentrations were estimated using a Seal Analytical AA3 HR
265   Nutrient Autoanalyzer. A detailed description of the instrument and specific procedures of the
266   analyses for each nutrient compound can be accessed at http://www.soest.hawaii.edu/S-
267   LAB/equipment/slab_autoanalyzer.htm.
268
269   *Biotic Factor Measurement*
270   Colony visual assessments were conducted every 2-3 days during the acclimation and
271   heating phase. Visual assessment methodology was modeled from Jokiel & Coles (1974), which
272   has since been used in modern studies (e.g., Coles et al. (2018)) and utilizes four visual categories
273   to describe the partial condition(s) of individual colonies: normal, pale, bleached, and dead (Fig.
274   4). Colonies were carefully handled underwater to examine the colony's entire surface, from which

275   partial percentages of each condition were recorded (e.g., 0% normal, 40% pale, 40% bleached,
276   20% dead). If distinction between bleached and dead condition was unclear, a magnifying glass
277   was used to determine polyp presence or absence. Other notable changes in condition were also
278   documented, such as the percent of surface area tissue loss by disease, predation (Protestomia
279   flatworms), or other parasitic organisms (e.g., algae, sponge, crab). 8% of *M. capitata* colonies
280   were removed due to severe predator infestation that resulted in >20% tissue loss. Colonies with
281   afflictions such as these were not included in any results or analyses.
282   The calcification rate of each coral colony was evaluated at the end of the acclimation and
283   heating phases. Calcification rate was measured using the buoyant weight technique described by
284   Jokiel et al. (1978). Organisms that could affect colony weight (e.g., sponges, crabs, algae) were
285   recorded then gently removed with seawater using a plastic syringe before measurement. Any
286   broken coral fragments were also recorded and weighed with the colony. The measured colony
287   weights were then converted to dry skeletal weights following procedures developed in Jokiel et
288   al. (1978). Final calcification rate (mm/day) for a given phase was calculated as the cube-root of
289   the difference in dry weights from initial to final measurements. From this method, calcification
290   rate was expressed as a change in colony radial length as opposed to a simple change in weight,
291   which allows for assessment of colony calcification differences irregardless of corallum size and
292   morphology (Maragos 1978).
293
294   *Statistical Approach*
295   R (Version 3.6.2) and the integrated development environment, R-Studio Desktop (Version
296   1.1.453, RStudio PBC, Boston, MA, USA), were used for all data analyses (R Core Team 2013).
297   Significance level was set at $\alpha = 0.05$ for all analyses. Graphs depicting coral survivorship, partial
298   mortality, and partial bleaching were created using Microsoft Excel. All other graphs were created
299   using R. Tank 8 (NH) was excluded from all abiotic and biotic data analysis due to malfunctioning
300   of its temperature control systems. Furthermore, a total of 10 colonies with > 30% predation of
301   surface area were also removed from data analysis: A (6), N (1), NH (1), and H (2). A summary
302   of sample sizes used in each biotic analysis are shown by phase, species, and treatment in Table
303   S1.
304   Temperature data from 30-min intervals during the heating phase were compared between
305   treatment groups to assess the effectiveness of artificial heating. Data were natural-log transformed
306   to meet the assumption of normality and differences by treatment assessed using a one-way
307   Analysis of Variance (ANOVA). *Post hoc* comparisons between treatment groups were
308   subsequently evaluated by comparing Bonferroni-adjusted model estimated marginal means
309   (EMMs) using the R package *emmeans* (Lenth et al. 2020).
310   The mean concentrations of nitrate + nitrite, phosphate, and ammonium from field sites
311   (Intake Pipe and South Bay) were compared to those of the ambient nutrient group (A) over the
312   entire study period (acclimation + heating phase). Homogeneity of variance for each nutrient was
313   determined using Levene's tests via the R package *car* (Fox & Weisberg 2019). One-way standard
314   or Welch's ANOVAs, depending on the presence of homoskedasticity, were then used to compare
315   differences in means between field sites and ambient mesocosm concentrations. Equivalent
316   techniques were applied for pairwise comparisons between all mesocosm treatment groups during
317   each phase. The mean concentrations of every nutrient type were also compared between
318   aggregated ambient (A + H) and nutrient enriched (N + NH) treatment groups during the heating
319   phase to confirm nutrient elevation during the experimental period. Unpaired two-tailed *t*-tests

320   were used to compare these differences in means, with homoscedasticity assessed prior via
321   Levene's tests.
322   Flow rate data were averaged by tank over the entire study period and were found to be
323   heteroskedastic. As such, analysis of flow rate differences between tanks was performed using a
324   Welch's one-way ANOVA, which does not assume equal variance between study groups (Welch
325   1951). A Games-Howell (GH) *post hoc* test was utilized to compare individual contrasts in flow
326   rate between tanks using the R package *rstatix* (Kassambara 2021). Peristaltic pump rate over the
327   entirety of the study period was also compared between tanks using a Welch's one-way ANOVA,
328   although post-hoc comparison was not required.
329   Colonies were classified as dead when partial mortality was $\geq$ 95%. Binary survivorship
330   data (1 = alive, 0 = dead) from the end of the heating phase and recovery phases were then
331   compared using binomial generalized linear models (GLMs) with cloglog link functions and bias-
332   reduced adjustments. The bias-reduced adjustment method is useful for binary data that show total
333   or near complete uniformity in one or more factor levels, which occurred for some treatment
334   groups with 100% or 0% survivorship and is available through the R package *brglm2* (Kosmidis
335   2017). Model factors used in binomial GLMs were coral species and treatment group, with *post*
336   *hoc* contrasts between treatment groups compared among species using Bonferroni-adjusted
337   EMMs. Model viability as compared to null models was assessed using Likelihood Ratio tests
338   from the R package *lmtest* (Hothorn et al. 2020).
339   Colony partial bleaching and partial mortality proportion data at the end of the heating
340   phase were modeled by beta regressions with logit link functions using coral species and treatment
341   group as model factors. Proportion data were transformed using Equation 1 (Smithson & Verkuilen
342   2006) in order to account for zero and one data points, which cannot be incorporated into beta
343   regressions. Equation variables *n* and *y* represent sample size and an untransformed proportion
344   value, respectively.
345

346
$$t(y) = \frac{y * (n - 1) + 0.5}{n}$$

347
348   Model viability as compared to null models were assessed using Likelihood Ratio tests and *post*
349   *hoc* contrasts between treatment groups evaluated among species using Bonferroni-adjusted
350   EMMs.
351   Days to bleaching (DTB) was determined as the number of days from the beginning of the
352   heating phase to when colony partial bleaching reached $\geq$ 95%. No colonies from A and N
353   treatment groups surpassed this threshold during the heating phase, thus DTB was only compared
354   between NH and H. Unpaired Wilcoxon Rank-Sum tests were used to compare ranked DTB data
355   between treatments among each species. Days to Mortality (DTM), which was defined
356   equivalently but instead in terms of partial mortality ($\geq$ 95% cutoff), was also assessed using these
357   statistical techniques.
358   Colony calcification data for all coral species were evaluated as the difference in mean
359   calcification rate from the end of acclimation phase to the end of heating phase (referred to as
360   "calcification-*d*"). Colonies with $\geq$50% partial mortality were excluded from statistical
361   calcification comparisons due to the potential of dissolution. Mean calcification-*d* was compared
362   between treatment groups using a Linear Mixed Effect model with species as a fixed effect and
363   treatment as both fixed and random. Viability of models were confirmed through assessment of

364 residual plots. *Post hoc* differences between treatments were compared among species using FDR-
365 adjusted EMMs.
366   Visual assessment data were assessed during Day 12 to examine corals near the
367 experimental mid-point and reassessed at the end of the heating phase (Day 31). Individual
368 colonies were assigned a single visual condition (i.e., normal, pale, bleached, or dead) determined
369 by their most prominent visual condition. The proportions of specific visual assessment levels were
370 assessed between pairs of treatment groups for each species. These comparisons were executed
371 using a Chi-Squared Test of Proportions with Yates' continuity correction, which is available
372 through base R. To accompany quantitative and statistical analyses of visual assessment data,
373 Multiple Correspondence Analyses (MCAs), which, similar to Principal Component Analyses,
374 organize categorical variables in multidimensional factor space, were used to compare the
375 explanatory contribution of different factor levels to spatial variation in data. MCAs were created
376 and plotted using the R package *FactoMineR* (Lê et al. 2008).
377
378 **Results**
379 *Environmental & Abiotic Parameters*
380   Mean temperature varied by phase and treatment group (Two-way ANOVA, $F_{(3, 51213)}$ =
381 13208, $p \le 0.001$). Temperature in heat-treated groups exceeded 30 °C for > 83% of the entire
382 heating phase, as compared to only ~4% in ambient heat groups. After excluding heat-treated
383 groups from the heating phase, temperature increased by an average of 0.48 °C from the
384 acclimation phase to the heating phase. This nearly half degree C elevation in ambient water
385 temperature over summer months coincided with seasonal changes in temperature associated with
386 prolonged daylight and irradiance. It also occurred just prior to the 2019 bleaching event that
387 peaked two months following the termination of this study. The island of Oʻahu experienced the
388 lowest degree heating weeks (0.5 °C) during 2019 (Winston 2022). Ambient temperatures did not
389 exceed coral thermal thresholds during the experiment as evidenced by the lack of bleaching for
390 corals under ambient conditions.
391   There were no observed differences in the mean concentrations of any nutrient type
392 between field sites (South Bay and Intake Pipe) and the ambient mesocosms (A) over the entirety
393 of the study period (Table S2), suggesting successful alignment of field and mesocosm nutrient
394 conditions. When aggregating mesocosm nutrient treated (N + NH) and non-treated (A + H)
395 groups, phosphate, nitrate + nitrite, and ammonium concentrations were on average 0.61 μM (*t*-
396 test, T = 4.42, df = 48, $p \le 0.001$), 0.56 μM (*t*-test, T = 7.59, df = 36, $p \le 0.001$), and 0.75 μM (*t*-
397 test, T = 6.74, df = 37, $p \le 0.001$) higher in enriched tanks, respectively, over the entirety of the
398 study period. Comparisons of mean concentrations between all individual treatment groups are
399 shown in Table S3.
400   Few differences in nutrient concentrations among nutrient enriched and ambient treatment
401 groups were observed during specific phases. Mean ammonium concentration during the
402 acclimation phase was greater in A than in H (*t*-test, T = 2.74, df = 7, $p = 0.03$) as well as in N than
403 in NH (*t*-test, T = 2.49, df = 6, $p = 0.05$). During the heating phase, mean phosphate concentration
404 was higher in H than in A (*t*-test, T = -2.79, df = 19, $p = 0.01$). Mean concentrations of all nutrient
405 types by phase and treatment groups are shown in Table 2.
406   Mean flow rates (sec/10 L) were compared between individual tanks over the entire study
407 period. The only significant differences in mean flow rates were between Tank 7 and Tanks 1
408 (Games-Howell, $p = 0.01$), 2 (Games-Howell, $p = 0.004$), and 12 (Games-Howell, $p \le 0.001$),
409 although the mean increase in flow rate by Tank 7 only ranged from 8.4 - 9.8 sec/10L (Welch's

410   One-way ANOVA, $F_{(10, 297)}$ = 3.96, $p \leq 0.001$). All tanks had mean flow rates lower than 60
411   sec/10L (< 60 min per complete turnover) in accordance with methods stipulated by Jokiel et al.
412   (2008) (Table S4).
413   The peristaltic pump rate (mL/min) of nutrient input into individual mesocosm tanks was
414   also assessed over the entire study period. There were no differences in pump rate between any
415   tanks, as mean rates ranged from only 3.17 – 3.24 mL/min (Table S5).
416
417   *Survivorship & Partial Mortality*
418   Coral survivorship and colony partial mortality did not differ by treatment group at the end
419   of the heating phase. The lowest observed survivorships were *P. acuta* (84%) and *L. scutaria*
420   (85%) in NH treatment groups (Table S6); mean partial mortality also reached as high as 22.4%
421   and 21.3% in H and NH *P. acuta* colonies, respectively, although these changes were not
422   significantly different from other conspecific treatments groups (Table S7).
423
424   *Partial Bleaching*
425   Partial bleaching was assessed over the course of the heating phase as a more sensitive
426   measure than total and partial mortality due to low mortality at the end of the heating phase (Fig.
427   5). Partial bleaching at the end of the heating phase varied by treatment group (Beta Regression
428   Model, pseudo-R^2 = 0.74, $Z_{(13, 314)}$ = 215.74, $p \leq 0.001$) but not by species. For all species, partial
429   bleaching was higher in NH and H treatments than in A and N treatments (EMMs, see S8). There
430   were no differences in partial bleaching among unheated groups (A and N) and heated groups (NH
431   and H), except for *L. scutaria*, which showed higher partial bleaching in H than in NH (EMM, *p*
432   ≤ 0.001, Table S8).
433
434   *Days to Bleaching / Mortality*
435   DTB was not assessed in A and N treatment groups as no colonies reached the $\geq$ 95%
436   partial bleaching threshold that was selected to constitute full colony bleaching. Among heat
437   treated groups, however, DTB was lower in H than it was in NH for all species (Wilcox Test, *p* <
438   0.05 for all comparisons, Table S9). On average, bleaching began 3.4 days earlier in H treatment
439   group colonies as compared to those of NH across all species.
440   No coral mortality occurred in the ambient nutrient group (N) and only one colony (*M.*
441   *capitata*) died under ambient conditions (A), thus DTM was not evaluated for N and A treatment
442   groups. No significant differences in DTM were found between NH and H treatment groups among
443   any species (Table S10).
444
445   *Calcification Rate*
446   The change in calcification rate (calcification-*d*) from the end of the acclimation phase to
447   the end of the heating period was also assessed between treatment groups among species. Minor
448   changes at the end of heating period were observed for ambient heating groups, although overall
449   decreases in calcification rate occurred for both NH and H (Fig. 6). Calcification-*d* in A and N
450   treatment groups was higher than calcification-*d* in H treatment groups among all species (EMMs,
451   *p* < 0.05 for all comparisons, Table S11), with no differences detected between the A and N control
452   groups. Calcification-*d* differences between both control groups (A and N) and NH were found in
453   *M. capitata* colonies (EMMs, *p* < 0.05 for both comparisons, Table S11), as calcification-*d* in the
454   NH treatment group was only marginally greater than that of the H treatment group. There were
455   no significant differences between H and NH treatment groups for *L. scutaria* and *M. capitata*,

456   although calcification-*d* was lower in H than in NH for *P. acuta* colonies (EMM, $p \leq 0.001$, Table
457   S11). These findings placed NH as an intermediate treatment group between ambient heat groups
458   and H with respect to calcification-*d* despite the overall decrease in calcification rate at the end of
459   the heating period in all species (Fig. 6).
460
461   *Visual Assessments*
462   By Day 12, the proportion of paled colonies in H treatment groups were greater than those
463   in all other treatment groups across every species (Chi-Squared Tests, $p < 0.05$ for all comparisons,
464   Table S12), except between NH and H treatment groups of *P. acuta*. Despite this, however, 83%
465   of *P. acuta* H colonies were either paled, bleached, or dead, as compared to 53% in NH colonies.
466   For all species, the percentage of normal colonies did not differ between A and NH treatment
467   groups, whereas normal colony percentage was greater in N than in A and NH treatment groups
468   excluding *P. acuta* (Chi-Squared Tests, $p < 0.05$ for all comparisons, Table S12). Percentages of
469   visual assessments by treatment and species are shown in Figure 7.
470   The Multiple Correspondence Analysis of visual assessments from Day 12, which
471   explained 35.3% of total variation, demonstrated several of the same quantitative patterns in
472   Euclidean space. Treatment groups N and H were distinctly separated in first dimensional space
473   (x-axis), whereas A and NH were located at an intermediate distance (Fig. 8, see Table S13 for
474   exact coordinates). These spatial trends were driven by normal and pale colonies, which explained
475   21.7% and 21.0% of first-dimension variation, with the normal condition centered negatively and
476   the pale condition centered positively. Coral species contributed minimally to variation and was
477   centered similarly for each species.
478   At the end of the heating period (Day 31), the bleached colony percentage of *L. scutaria*
479   was lower in NH than in H (Chi-Squared Test, $\chi^2 = 10.09$, df $= 1$, $p \leq 0.001$), whereas no differences
480   in the *M. capitata* and *P. acuta* colonies of these treatment groups were observed (Table S14. The
481   percentage of paled colonies of *L. scutaria* was also lower in the N than the A treatment groups
482   (Chi-Squared Test, $\chi^2 = 8.42$, df $= 1$, $p = 0.004$), although this was again not observed for other
483   species. Altogether, there were no recorded bleached or dead colonies in the A and N treatment
484   groups (Fig. S1).
485   The MCA of visual assessments from the end of the heating period well represented data
486   in two-dimensional space (41.3% cumulatively, Fig. S2) and visualized similar trends as were
487   described above. The model's first dimensional space showed separation of heated and non-heated
488   treatment groups, which was driven predominantly by the normal and bleached conditions (see
489   Table S15 for exact coordinates). Alternatively, the variation in second-dimensional space was
490   primarily determined by the pale condition, with the A and NH treatment group centered more
491   positively. This may be concomitant with the lower percentage of bleached corals in NH than in
492   H of *L. scutaria* colonies (Fig. S1), which may instead only have paled, suggesting this trend may
493   be driven only by *L. scutaria*. Indeed, there were differences in species position in second-
494   dimensional space, with *L. scutaria* more positively centered in comparison with other species.
495
Discussion
497   In all examined coral species, enrichment of heat-stressed colonies with low levels of
498   inorganic phosphorus and nitrogen concentrations resulted in improvements of coral conditions
499   indicative of maintaining the host and endosymbiont relationship. In this study, we conducted
500   mesocosm-based experiments on coral exposure to minimal balanced nutrient enrichment (<1 µM
501   of nitrogen and phosphorous) during a prolonged heating event (31 days), which are becoming

502   increasingly common in sub-tropical environments such as the Hawaiian Islands. We assessed
503   colony growth and various coral conditions over the study period (i.e., survivorship, partial
504   mortality and bleaching, bleaching progress), finding evidence of ameliorated growth rates and
505   delayed bleaching in colonies subjected to thermal stress and nutrient enrichment. For all species
506   tested, the onset of bleaching was delayed by 3.4 days in nutrient-enriched and heated colonies as
507   compared to heated-only colonies, which was likely due to the reduction in paled individuals
508   midway through the heating period (Fig. 7). Relatedly, bleaching was consistently lower
509   proportionally in nutrient-enriched *L. scutaria* and *M. capitata* colonies during the heating period
510   (Fig. 5), albeit a lack of statistical difference during the final day of heating. This study is the only
511   published account of prolonged coral exposure (>30 days) to elevated temperature and minimal
512   balanced nutrient enrichment, expanding on shorter duration studies (e.g., Ezzat et al. 2016;
513   Hadjioannou et al. 2019; Tanaka et al. 2014) to investigate chronic exposure, which may more
514   closely resemble thermal events in the field.
515   Calcification rate, which was used as a proxy for host bioenergetic and metabolic status,
516   was also less affected in nutrient-enriched groups during heat stress. The enhancement of host
517   metabolism under enriched nutrient conditions has been recorded in previous studies (Beraud et
518   al. 2013; Fabricius 2005; Tanaka et al. 2007) and may help to explain relatively lower calcification
519   rates of NH as compared to H treatment groups observed in this study. Altogether, these results
520   suggest that minor and balanced nutrient enrichments can increase the resilience of individual
521   colonies to thermal stress during heating events.
522   The implementation of Multiple Correspondence Analyses (MCA) to visualize patterns in
523   categorical datasets has been utilized in ecological studies (e.g., Aubert et al. 2006; D'Onghia et
524   al. 2011), although it remains somewhat irregular as oftentimes biological sampling predominantly
525   generates numerical response data. Here, however, our visual assessments were modeled after
526   techniques employed by Jokiel & Coles (1977) and subsequently Coles et al. (2018), which permit
527   the rapid and practical evaluation of the bleached status of large numbers of coral colonies every
528   2-3 days, producing categorical data. The combination of descriptive MCA plots with subsequent
529   chi-squared proportional tests allowed for visual and statistical interpretation of these data. This
530   approach revealed that nutrient enrichment decreased bleaching of heated colonies during the
531   intermediate stage (Day 12) of the heating period. By the end of heating (Day 31), the nutrient-
532   enriched heated group had higher proportions of paled colonies than did the heated group, which
533   were instead primarily bleached or dead. These indications of remediated health in nutrient-treated
534   groups at the end of heating are mostly attributed to *L. scutaria*, however, as paled colony
535   proportion did not vary significantly among other species.
536   The delayed decline in colony visual conditions may be tied to the qualitative observation
537   of greater zooxanthellate density in nutrient-enriched colonies in both heated and unheated groups.
538   Although over-proliferation of microalgal symbionts under high and unbalanced nutrient
539   enrichment has been shown to exacerbate bleaching (D'Angelo & Wiedenmann 2014; Rosset et
540   al. 2017; Wooldridge & Done 2009), the modest concentrations of balanced nutrient enrichment
541   in this study may have been too low to cause overgrowth and thus minimized any associated
542   negative effects. This aligns with expectations expressed by D'Angelo & Wiedenmann (2014) who
543   proposed that N/P concentrations may only be harmful under imbalanced ratios. This interpretation
544   is further supported by new evidence that endosymbionts can maintain stable host-symbiont
545   nutrient relationships during modest fluctuations in density due to alterations in symbiont
546   photophysiology (Krueger et al. 2020). Although we lack measurements of causal variables such
547   as photosynthetic rate or cellular nutrient composition that could confirm these conditions, the

548 nutrient concentrations in our mesocosm experiments were similar to measurements recorded by
549 Becker et al. (2021) in their field manipulation study, which observed increases in gross
550 photosynthetic rate and maximal performance. Our observations of mollified calcification rates
551 may also be indicative of host metabolic mitigation as past studies have observed greater skeletal
552 extension of corals when enriched with phosphate (Dunn et al. 2012; Shantz & Burkepile 2014),
553 although the structural integrity of new growth may be compromised. As such, the presence of
554 phosphate in our nutrient treatments may have been the main driver of observed improvements to
555 visual health and calcification rate due to sufficient supply of phosphate for prevention of P-
556 limitation (D'Angelo & Wiedenmann 2014), whereas the negative effects from nitrate and nitrite
557 may have been minimized or otherwise influenced by the presence of ammonium (Ezzat et al.
558 2016; Marangoni et al. 2020). The duration of positive effects from phosphate introduction is
559 unclear, however, as bleaching was quite pervasive by the end of the heating period.

560   Several past studies have summarized potential mechanisms for augmented coral resiliency
561 in response to chronic or multiple acute disturbance events (Suggett et al. 2017; Torda et al. 2017).
562 This "ecological memory" (see Hackerott et al. 2021; Hughes et al. 2019) approach is a leading
563 rationale supporting current and future individual and community-level resiliency in the context
564 of anthropogenic stressors. Tolerance to higher temperatures and reduced water quality, for
565 example, have been observed in reef habitats over generational scales (Coles et al. 2018;
566 Tisthammer et al. 2021), with more recent studies suggesting that rapid thermal acclimatization
567 may occur in response to acute environmental stresses through non-genetic inheritance, epigenetic
568 adaptation, and microbiome plasticity (Littman et al. 2011; Palumbi et al. 2014; Putnam 2021).
569 Kāneʻohe Bay, which was historically highly suitable for reef coral growth (Edmondson 1928),
570 entered a period of severe coral decline after introduction of major high-nutrient sewage output in
571 1963. After the majority of sewage flow was removed in 1978, Kāneʻohe Bay underwent a reverse
572 phase-shift to a coral dominant regime over the next several decades (Smith et al. 1981). Initial
573 coral recovery was relatively immediate, with reported increases in coral cover of 26% within
574 several years of effluent removal (Smith et al. 1981). It has also been suggested that corals in
575 Kāneʻohe Bay have developed improved thermal tolerance due to the incumbent high temperatures
576 relative to adjacent reefs (Coles et al. 2018; Jury & Toonen 2019) and, when considering nutrient
577 history in tandem, may have the potential for improved tolerance to combined nutrient and heat
578 augmentation. Accordingly, nutrient history has recently been shown to mediate the response of
579 Scleractinian corals to thermal stress (Hadjioannou et al. 2019).
580   The differential responses to heat stress by the three coral species in this study with respect
581 to visual assessment, calcification rate, and partial mortality and bleaching may be due to
582 differences in life history, morphology, and stress tolerance. *P. acuta*, which declined rapidly in
583 visual status and partial mortality, also demonstrated the greatest decrease and variation in
584 calcification rate when exposed to heat stress and nutrient enrichment (Fig. 6). General trends
585 suggest that *L. scutaria* may be more tolerant to thermal stress (Bahr et al. 2016; Coles et al. 2018)
586 with and without nutrient enrichment, as these colonies exhibited less bleaching during the
587 intermediate periods of the heating phase and showed no statistical differences in calcification rate
588 between the NH treatment group and ambient groups. When considering variation in response,
589 factors that could contribute to species-specific performance are heterotrophic feeding plasticity
590 and endosymbiont regulation. Coral heterotrophic feeding has been recognized as one of the main
591 sources for energy acquisition during stressed conditions, especially under disruption of
592 endosymbiont autotrophy (i.e., bleaching) (Grottoli et al. 2006). Greater reliance on heterotrophic
593 feeding can alleviate bleaching and maintain coral growth by fulfilling carbon demand that is lost

594   from the breakdown of symbiosis (Houlbrèque & Ferrier-Pagès 2009). A recent study by Price et
595   al. (2021) suggested that the average contribution of heterotrophy to Hawaiian coral feeding is
596   approximately 20-50%, depending on the species. The level of heterotrophic feeding was likely
597   variable among the coral species examined in this study and may have confounded the magnitude
598   of responses to heat stress. Indeed, our results showed delayed bleaching (Days to bleaching, DTB)
599   was more pronounced in *M. capitata* (Fig. 5, Table S9), the species with the highest heterotrophic
600   feeding rate during post-bleaching recovery. This concurs with other studies that report *M. capitata*
601   was able to obtain up to 100% of the required metabolic energy requirements from heterotrophy
602   (Dobson et al. 2021; Grottoli et al. 2006). Alternatively, the relatively poor response of *P. acuta*
603   to heating in this study may have been driven by its limited ability to regulate endosymbiont
604   proliferation (Fox et al. 2021). These results imply that any positive effects of balanced nutrient
605   enrichment may be mediated by the stress tolerance of the affected species.
606   Our study presents evidence for possible bleaching mitigation under low-level nutrient
607   enrichment. Temperature, however, was unequivocally the dominant factor that induced
608   bleaching, considering there were clear differences in all measured parameters between ambient
609   (~28.5 °C) and heated (~30.7 °C) groups regardless of their nutrient regime. Although not
610   measured in this study, the Symbiodiniaceae genotype may have prompted differences in visual
611   conditions and calcification observed in this study, as several articles have shown thermal
612   tolerance differences between Symbiodiniaceae genotypes (Grégoire et al. 2017; Stat & Gates
613   2011). Moreover, the variations in nutrient uptake, carbon translocation rates, and nutrient
614   competition between Symbiodiniaceae genotype have been found (Baker et al. 2013), and it is
615   plausible that the Symbiodiniaceae species competition (dominance) could be altered under
616   nutrient enrichment due to differing nutrient processing capacities. The effect of nutrient
617   enrichment on Symbiodiniaceae competition and the impact on thermal tolerance requires further
618   investigation.
619   Although the utilization of a mesocosm study system can control for many factors that
620   cannot be regulated in traditional field studies, there remain some limitations. Adjustment of
621   nutrient inputs into enriched tanks required consistent modification, as uptake and release of
622   measured nutrient concentrations by corals continuously alters *in situ* tank concentrations. This led
623   to higher ranges in measurements, as was reflected in the standard error of nutrient concentrations,
624   although this is a common issue in nutrient manipulation studies (e.g., Fox et al. 2021) and did not
625   preclude statistically significant differences between enriched and ambient treatment groups.
626   Secondly, because mesocosms rely on proximate seawater influxes, the water temperature of
627   ambient tanks during the heating period rose on average to sub-lethal levels (~28.5 °C).
628   Interestingly, however, little paling or bleaching was observed in nutrient-enriched ambient-
629   temperature colonies as compared to fully ambient colonies (Fig. S1), which is consistent with
630   observations by McClanahan et al. (2003) that fertilizer enrichment precluded typical summer
631   bleaching. As such, the mitigative potential of nutrient enrichment in this study may also apply to
632   corals experiencing sub-lethal temperature exposure.
633
634   **Conclusions**
635   Despite clear negative feedbacks of eutrophication on reef degradation (Littler & Littler
636   1984; Wooldridge 2013), deciphering the effects of direct nutrient enrichment on coral thermal
637   tolerance has been a convoluted and ambiguous initiative for several decades. Dissolved inorganic
638   nutrients should be treated as a "double-edged sword" that can alter coral holobiont symbioses
639   (Wooldridge 2013). Many studies have found that excess nitrogen can exacerbate bleaching in

640 field and laboratory settings (e.g., Burkepile et al. 2020; Chumun et al. 2013; Nordemar et al.
641 2003). In this context, both nutrient identity and N:P ratio have been identified as controlling
642 factors influencing coral response (Ezzat et al. 2015; Marangoni et al. 2020; Rosset et al. 2017;
643 Wiedenmann et al. 2013). Therefore, the conditions and threshold that balances beneficial and
644 harmful impacts of nutrients on coral is crucial to elucidate for near-shore management and
645 maintenance of healthy reef ecosystems in a changing ocean. Although critiques of past studies
646 have posited that coral exposure to large N:P ratios and (or) concentrations does not occur in
647 natural systems, recent studies have demonstrated that increases in N:P ratio at tested levels can
648 occur via anthropogenically driven nutrient enrichment or excessive runoff (Lapointe et al. 2020),
649 which has coincided with bleaching events (D'Angelo & Wiedenmann 2014; Lapointe et al. 2019).
650 While the importance of nutrient availability (N:P ratio) to coral thermal bleaching has been
651 discussed, the coral host can limit or stabilize the algal proliferation (Baird et al. 2009) and
652 thresholds of nutrient concentrations and (or) N:P ratios that balance the presence of mutualism
653 and parasitism have not yet been ubiquitously identified. Here, we presented novel results that
654 infer low and balanced nutrient enrichment during thermal stress may mitigate coral bleaching
655 during the early stages of a heating event and help to maintain mutualism. Our findings seemingly
656 align with those of Becker et al. (2021) and are particularly relevant considering many reef systems
657 are experiencing sustained or increased anthropogenic nutrient input from sources such as fertilizer
658 and sewage outfall, which can lead to macroalgal overproliferation and associated coral mortality.
659 Determining the remediatory potential of this approach across different spatial scales will require
660 similar mesocosm or field studies in other reef systems that consider local nutrient dynamics, as
661 Kāneʻohe Bay is unique in its nutrient and temperature history.
662

663 **Acknowledgements**
664   This work builds upon the research foundation of Paul L. Jokiel, a pioneer in the field of
665 Marine Science. Contributions to experimental maintenance and design were made by Dr. Evelyn
666 Cox, Dr. Steve Coles, Andrew Graham, Anita Tsang, Sarah Severino and Yuko Stender of the
667 Coral Reef Ecology Laboratory at the Hawaiʻi Institute of Marine Biology. The authors would also
668 like to thank Dr. Jake Ferguson for his guidance regarding several statistical techniques.
669 HIMB contribution number: 1884
670 SOEST contribution number: 11490
671

672 **References**
673 Adam TC, Burkepile DE, Holbrook SJ, Carpenter RC, Claudet J, Loiseau C, Thiault L, Brooks
674   AJ, Washburn L, and Schmitt RJ. 2021. Landscape-scale patterns of nutrient enrichment
675   in a coral reef ecosystem: implications for coral to algae phase shifts. *Ecological*
676   *Applications* 31:e02227.
677 Anthony K, Connolly SR, and Hoegh-Guldberg O. 2007. Bleaching, energetics, and coral
678   mortality risk: Effects of temperature, light, and sediment regime. *Limnology and*
679   *oceanography* 52:716-726.
680 Aubert M, Margerie P, Ernoult A, Decaens T, and Bureau F. 2006. Variability and heterogeneity
681   of humus forms at stand level: Comparison between pure beech and mixed beech-
682   hornbeam forest. *Annals of Forest Science* 63:177-188.
683   https://doi.org/10.1051/forest:2005110

684   Bahr KD, Jokiel PL, and Rodgers KS. 2016. Relative sensitivity of five Hawaiian coral species
685   to high temperature under high-pCO2 conditions. *Coral Reefs* 35:729-738.
686   10.1007/s00338-016-1405-4
687   Baird AH, Bhagooli R, Ralph PJ, and Takahashi S. 2009. Coral bleaching: the role of the host.
688   *Trends in Ecology & Evolution* 24:16-20. 10.1016/j.tree.2008.09.005
689   Baker DM, Andras JP, Jordán-Garza AG, and Fogel ML. 2013. Nitrate competition in a coral
690   symbiosis varies with temperature among Symbiodinium clades. *The International*
691   *Society for Microbial Ecology Journal* 7:1248-1251.
692   Becker DM, Putnam HM, Burkepile DE, Adam TC, Vega Thurber R, and Silbiger NJ. 2021.
693   Chronic low-level nutrient enrichment benefits coral thermal performance in a fore reef
694   habitat. *Coral Reefs* in-press:1-19.
695   Beraud E, Gevaert F, Rottier C, and Ferrier-Pages C. 2013. The response of the scleractinian
696   coral Turbinaria reniformis to thermal stress depends on the nitrogen status of the coral
697   holobiont. *Journal of Experimental Biology* 216:2665-2674.
698   Bongiorni L, Shafir S, Angel D, and Rinkevich B. 2003. Survival, growth and gonad
699   development of twohermatypic corals subjected to in situfish-farmnutrient enrichment.
700   *Marine Ecology Progress Series* 253:137-144.
701   Burkepile DE, Shantz AA, Adam TC, Munsterman KS, Speare KE, Ladd MC, Rice MM, Ezzat
702   L, McIlroy S, Wong JCY, Baker DM, Brooks AJ, Schmitt RJ, and Holbrook SJ. 2020.
703   Nitrogen identity drives differential impacts of nutrients on coral bleaching and mortality.
704   *Ecosystems* 23:798-811. 10.1007/s10021-019-00433-2
705   Carlson RR, Foo SA, and Asner GP. 2019. Land use impacts on coral reef health: a ridge-to-reef
706   perspective. *Front Mar Sci* 6. 10.3389/fmars.2019.00562
707   Chumun PK, Casareto BE, Higuchi T, Irikawa A, Bhagooli R, Ishikawa Y, and Suzuki Y. 2013.
708   High nitrate levels exacerbate thermal photo-physiological stress of zooxanthellae in the
709   reef-building coral Pocillopora damicornis. *Eco-Engineering* 25:75-83.
710   Coles SL, Bahr KD, Rodgers KUS, May SL, McGowan AE, Tsang A, Bumgarner J, and Han JH.
711   2018. Evidence of acclimatization or adaptation in Hawaiian corals to higher ocean
712   temperatures. *PeerJ* 6:e5347. 10.7717/peerj.5347
713   Coles SL, Jokiel PL, and Lewis C. 1976. Thermal tolerance in tropical versus sub-tropical reef
714   corals. *Pacific Science* 30:159-166.
715   Cunning R, and Baker AC. 2013. Excess algal symbionts increase the susceptibility of reef
716   corals to bleaching. *Nat Clim Change* 3:259-262.
717   D'Angelo C, and Wiedenmann J. 2014. Impacts of nutrient enrichment on coral reefs: new
718   perspectives and implications for coastal management and reef survival. *Current Opinion*
719   *in Environmental Sustainability* 7:82-93.
720   D'Onghia G, Indennidate A, Giove A, Savini A, Capezzuto F, Sion L, Vertino A, and Maiorano
721   P. 2011. Distribution and behaviour of deep-sea benthopelagic fauna observed using
722   towed cameras in the Santa Maria di Leuca cold-water coral province. *Marine Ecology*
723   *Progress Series* 443:95-110. 10.3354/meps09432
724   Dobson KL, Ferrier-Pages C, Saup CM, and Grottoli AG. 2021. The Effects of Temperature,
725   Light, and Feeding on the Physiology of Pocillopora damicornis, Stylophora pistillata,
726   and Turbinaria reniformis Corals. *Water* 13:2048. https://doi.org/10.3390/w13152048
727   Donovan MK, Adam TC, Shantz AA, Speare KE, Munsterman KS, Rice MM, Schmitt RJ,
728   Holbrook SJ, and Burkepile DE. 2020. Nitrogen pollution interacts with heat stress to

production

272

773   Grover R, Maguer J-F, Allemand D, and Ferrier-Pagés C. 2003. Nitrate uptake in the
774   scleractinian coral Stylophora pistillata. *Limnology and oceanography* 48:2266-2274.
775   10.4319/lo.2003.48.6.2266
776   Grover R, Maguer J-FO, Allemand D, and Ferrier-PagèS C. 2008. Uptake of dissolved free
777   amino acids by the scleractinian coral Stylophora pistillata. *Journal of Experimental*
778   *Biology* 211:860-865. 10.1242/jeb.012807
779   Hackerott S, Martell HA, and Eirin-Lopez JM. 2021. Coral environmental memory: causes,
780   mechanisms, and consequences for future reefs. *Trends in Ecology & Evolution* 36:1011-
781   1023. https://doi.org/10.1038/s41558-018-0351-2
782   Hadjioannou L, Jimenez C, Rottier C, Sfenthourakis S, and Ferrier-Pages C. 2019. Response of
783   the temperate scleractinian coral Cladocora caespitosa to high temperature and long-term
784   nutrient enrichment. *Scientific Reports* 9:14229. https://doi.org/10.1038/s41598-019-
785   50716-w
786   Hoegh-Guldberg O, Jacob D, Taylor M, Bolaños TG, Bindi M, Brown S, Camilloni IA,
787   Diedhiou A, Djalante R, and Ebi K. 2019. The human imperative of stabilizing global
788   climate change at 1.5 C. *Science* 365. 10.1126/science.aaw6974
789   Hothorn T, Zeileis A, Cummins C, Millo G, and Mitchell D. 2020. lmtest: Testing linear
790   regression models. R.
791   Houlbrèque F, and Ferrier-Pagès C. 2009. Heterotrophy in tropical scleractinian corals.
792   *Biological Reviews* 84:1-17. 10.1111/j.1469-185X.2008.00058.x
793   Hughes TP, Kerry JT, Álvarez-Noriega M, Álvarez-Romero JG, Anderson KD, Baird AH,
794   Babcock RC, Beger M, Bellwood DR, Berkelmans R, Bridge TC, Butler IR, Byrne M,
795   Cantin NE, Comeau S, Connolly SR, Cumming GS, Dalton SJ, Diaz-Pulido G, Eakin
796   CM, Figueira WF, Gilmour JP, Harrison HB, Heron SF, Hoey AS, Hobbs J-PA,
797   Hoogenboom MO, Kennedy EV, Kuo C-Y, Lough JM, Lowe RJ, Liu G, McCulloch MT,
798   Malcolm HA, McWilliam MJ, Pandolfi JM, Pears RJ, Pratchett MS, Schoepf V, Simpson
799   T, Skirving WJ, Sommer B, Torda G, Wachenfeld DR, Willis BL, and Wilson SK. 2017.
800   Global warming and recurrent mass bleaching of corals. *Nature* 543:373-377.
801   10.1038/nature21707
802   Hughes TP, Kerry JT, Connolly SR, Baird AH, Mark Eakin C, Heron SF, Hoey AS,
803   Hoogenboom MO, Jacobson M, Liu G, Pratchett MS, Skirving WJ, and Torda G. 2019.
804   Ecological memory modifies the cumulative impact of recurrent climate extremes.
805   *Nature Climate Change* 9:40-43. https://doi.org/10.1038/s41558-018-0351-2
806   Hunter CL, and Evans CW. 1995. Coral reefs in Kaneohe Bay, Hawaii: Two centuries of
807   Western influence and two decades of data. *Bulletin of Marine Science* 57:501-515.
808   Iglesias-Prieto R, Matta JL, Robins WA, and Trench RK. 1992. Photosynthetic response to
809   elevated temperature in the symbiotic
810   dinoflagellate Symbiodinium microadriaticum in culture. *Proceedings of the National Academy*
811   *of Sciences* 89:10302-10305.
812   Johnston EC, Forsman ZH, and Toonen RJ. 2018. A simple molecular technique for
813   distinguishing species reveals frequent misidentification of Hawaiian corals in the genus
814   Pocillopora. *PeerJ* 6:e4355. 10.7717/peerj.4355
815   Jokiel PL, Bahr KD, and Rodgers KS. 2014. Low-cost, high-flow mesocosm system for
816   simulating ocean acidification for CO2 gas. *Limnol Oceanogr Methods* 12:313-322.

817 Jokiel PL, and Brown EK. 2004. Global warming, regional trends and inshore environmental
818   conditions influence coral bleaching in Hawaii. *Global change biology* 10:1627-1641.
819   10.1111/j.1365-2486.2004.00836.x
820 Jokiel PL, and Coles SL. 1974. Effects of heated effluent on hermatypic corals at Kahe Point,
821   Oahu. *Pacific Science* 28:1-18.
822 Jokiel PL, and Coles SL. 1977. Effects of temperature on the mortality and growth of Hawaiian
823   reef corals. *Mar Biol* 43:201-208. 10.1007/BF00402312
824 Jokiel PL, Maragos J, and Franzisket L. 1978. Coral growth: buoyant weight technique. In:
825   Johannes RE, ed. *Coral reefs: research methods; monographs on oceanographic*
826   *methodology*. Paris: Unesco, 529-542.
827 Jokiel PL, Rodgers KS, Kuffner IB, Andersson AJ, Cox EF, and Mackenzie FT. 2008. Ocean
828   acidification and calcifying reef organisms: a mesocosm investigation. *Coral Reefs*
829   27:473-483.
830 Jury CP, and Toonen RJ. 2019. Adaptive responses and local stressor mitigation drive coral
831   resilience in warmer, more acidic oceans. *Proceedings of the Royal Society B: Biological*
832   *Science* 286. https://doi.org/10.1098/rspb.2019.0614
833 Kassambara A. 2021. rstatix: Pipe-friendly framework for basic statistical tests. R.
834 Kosmidis I. 2017. brglm2: Bias reduction in generalized linear models. R.
835 Krueger T, Hawkins TD, Becker S, Pontasch S, Dove S, Hoegh-Guldberg O, Leggat W, Fisher
836   PL, and Davy SK. 2015. Differential coral bleaching—Contrasting the activity and
837   response of enzymatic antioxidants in symbiotic partners under thermal stress.
838   *Comparative Biochemistry and Physiology Part A: Molecular & Integrative Physiology*
839   190:15-25.
840 Krueger T, Horwitz N, Bodin J, Giovani M-E, Escrig S, Fine M, and Meibom A. 2020.
841   Intracellular competition for nitrogen controls dinoflagellate population density in corals.
842   *Proceedings of the Royal Society B: Biological Science* 287:20200049.
843   http://dx.doi.org/10.1098/rspb.2020.0049
844 Kuffner I, Walters L, Becerro M, Paul V, Ritson-Williams R, and Beach K. 2006. Inhibition of
845   coral recruitment by macroalgae and cyanobacteria. *Marine Ecology Progress Series*
846   323:107-117. 10.3354/meps323107
847 Lapointe BE, Brewton RA, Herren LW, Porter JW, and Hu C. 2019. Nitrogen enrichment,
848   altered stoichiometry, and coral reef decline at Looe Key, Florida Keys, USA: a 3-decade
849   study. *Mar Biol* 166:108.
850 Lapointe BE, Herren LW, Brewton RA, and Alderman PW. 2020. Nutrient over-enrichment and
851   light limitation of seagrass communities in the Indian River Lagoon, an urbanized
852   subtropical estuary. *Science of the Total Environment* 699:134068.
853   10.1016/j.scitotenv.2019.134068
854 Laws EA, and Redalje DG. 1982. Sewage diversion effects on the water column of a subtropical
855   estuary. *Marine Environmental Research* 6:265-279.
856 Lê S, Josse J, and Husson F. 2008. FactoMineR: A package for multivariate analysis. *Journal of*
857   *Statistical Software* 25:1-18. 10.18637/jss.v025.i01
858 Lenth R, Singmann H, Love J, Buerkner P, and Herve M. 2020. emmeans: estimated marginal
859   means, aka least-squares means. 1.4.5 ed.
860 Lesser MP. 2006. Oxidative stress in marine environments: biochemistry and physiological
861   ecology. *Annual Review of Physiology* 68:254-278.
862   10.1146/annurev.physiol.68.040104.110001

863   Littler MM, and Littler DS. 1984. Relationships between macroalgal functional form groups and
864   substrata stability in a subtropical rocky-intertidal system. *Journal of experimental*
865   *marine biology and ecology* 74:13-34.
866   Littman R, Willis BL, and Bourne DG. 2011. Metagenomic analysis of the coral holobiont
867   during a natural bleaching event on the Great Barrier Reef. *Environmental Microbology*
868   *Reports* 3:651-660. 10.1111/j.1758-2229.2010.00234.x
869   Maragos J. 1978. Coral growth: geometrical relationships. In: Stoddart DR, and Johannes RE,
870   eds. *Handbook of coral reef research methods*. Paris: Unesco, 543-550.
871   Marangoni LF, Ferrier-Pages C, Rottier C, Bianchini A, and Grover R. 2020. Unravelling the
872   different causes of nitrate and ammonium effects on coral bleaching. *Scientific Reports*
873   10:11975.
874   Marubini F, and Davies PS. 1996. Nitrate increases zooxanthellae population density and
875   reduces skeletogenesis in corals. *Marine Biology* 127:319-328.
876   McClanahan TR, Sala E, Stickels PA, Cokos BA, Baker AC, Starger CJ, and Jones IV SH. 2003.
877   Interaction between nutrients and herbivory in controlling algal communities and coral
878   condition on Glover's Reef, Belize. *Marine Ecology Progress Series* 261:135-147.
879   McCook LJ, Jompa J, and Diaz-Pulido G. 2001. Competition between corals and algae on coral
880   reefs: a review of evidence and mechanisms. *Coral Reefs* 19:400-417.
881   Morris LA, Voolstra CR, Quigley KM, Bourne DG, and Bay LK. 2019. Nutrient availability and
882   metabolism affect the stability of coral-symbiodiniaceae symbioses. *Trends in*
883   *Microbiology* 27:678-689.
884   Muscatine L, Ferrier-Pages C, Blackburn A, Gates RD, Baghdasarian G, and Allemand D. 1998.
885   Cell-specific density of symbiotic dinoflagellates in tropical anthozoans. *Coral Reefs*
886   17:329-337.
887   Nordemar I, Nyström M, and Dizon R. 2003. Effects of elevated seawater temperature and
888   nitrate enrichment on the branching coral Porites cylindrica in the absence of particulate
889   food. *Marine Biology* 142:669-677. 10.1007/s00227-002-0989-0
890   Palumbi SR, Barshis DJ, Traylor-Knowles N, and Bay RA. 2014. Mechanisms of reef coral
891   resistance to future climate change. *Science* 344:895-898. 10.1126/science.1251336
892   Price JP, McLachlan RH, Jury CP, Toonen RJ, and Grottoli AG. 2021. Isotopic approaches to
893   estimating the contribution of heterotrophic sources to Hawaiian corals. *Limnology and*
894   *oceanography* 66:2393-2407. 10.1002/lno.11760
895   Putnam HM. 2021. Avenues of reef-building coral acclimatization in response to rapid
896   environmental change. *Journal of Experimental Biology* 224:jeb239319.
897   10.1242/jeb.239319
898   R Core Team. 2013. R: A language and environment for statistical computing. Vienna, Austria.
899   Rädecker N, Pogoreutz C, Gegner HM, Cárdenas A, Roth F, Bougoure J, Guagliardo P, Wild C,
900   Pernice M, and Raina J-B. 2021. Heat stress destabilizes symbiotic nutrient cycling in
901   corals. *Proceedings of the National Academy of Sciences* 118:e2022653118.
902   Ritson-Williams R, and Gates RD. 2020. Coral community resilience to successive years of
903   bleaching in Kāneʻohe Bay, Hawaiʻi. *Coral Reefs* 39:757-769. 10.1007/s00338-020-
904   01944-4
905   Rosset S, Wiedenmann J, Reed AJ, and D'Angelo C. 2017. Phosphate deficiency promotes coral
906   bleaching and is reflected by the ultrastructure of symbiotic dinoflagellates. *Mar Pollut*
907   *Bull* 118:180-187.

908 Shantz AA, and Burkepile DE. 2014. Context-dependent effects of nutrient loading on the coral-
909   algal mutualism. *Ecology* 95:1995-2005.
910 Smith DJ, Suggett DJ, and Baker NR. 2005. Is photoinhibition of zooxanthellae photosynthesis
911   the primary cuase of thermal bleaching in corals? *Glob Chang Biol* 11:1-11.
912 Smith SV. 1984. Phosphorus versus nitrogen limitation in the marine environment. *Limnology*
913   *and oceanography* 29:1149-1160.
914 Smith SV, Kimmerer WJ, Laws EA, R.E. B, and Walsh TW. 1981. Kaneohe Bay sewage
915   diversion experiment: Perspectives on ecosystem responses to nutritional perturbation.
916   *Pacific Science* 35:279-395.
917 Smithson M, and Verkuilen J. 2006. A better lemon squeezer? Maximum-likelihood regression
918   with beta-distributed dependent variables. *Psychological methods* 11:54.
919 Stambler N, Popper N, Dubinsky Z, and Stimson J. 1991. Effects of nutrient enrichment and
920   water motion on the coral Pocillopora damicornis. *Pacific Science* 45:299-307.
921 Stat M, and Gates RD. 2011. Clade D Symbiodinium in Scleractinian corals: A "nugget" of
922   hope, a selfish opportunist, an ominous sign, or all of the above? *Journal of Marine*
923   *Sciences* 2011:730715. 10.1155/2011/730715
924 Suggett DJ, Warner ME, and Leggat W. 2017. Symbiotic dinoflagellate functional diversity
925   mediates coral survival under ecological crisis. *Trends in Ecology & Evolution* 32:735-
926   745. 10.1016/j.tree.2017.07.013
927 Tanaka Y, Grottoli AG, Matsui Y, Suzuki A, and Sakai K. 2017. Effects of nitrate and phosphate
928   availability on the tissues and carbonate skeleton of scleractinian corals. *Marine Ecology*
929   *Progress Series* 570:101-112.
930 Tanaka Y, Hayashibara T, and Ogawa H. 2007. Imbalanced coral growth between organic tissue
931   and carbonate skeleton caused by nutrient enrichment. *Limnology and oceanography*
932   52:1139-1146.
933 Tanaka Y, Inoue M, Nakamura T, Suzuki A, and Sakai K. 2014. Loss of zooxanthellae in a coral
934   under high seawater temperature and
935 nutrient enrichment. *Journal of experimental marine biology and ecology* 457:220-225.
936   10.1016/j.jembe.2014.04.019
937 Tisthammer KH, Timmins-Schiffman E, Seneca FO, Nunn BL, and Richmond RH. 2021.
938   Physiological and molecular responses of lobe coral indicate nearshore adaptations to
939   anthropogenic stressors. *Scientific Reports* 11:3423. https://doi.org/10.1038/s41598-021-
940   82569-7
941 Torda G, Donelson JM, Aranda M, Barshis DJ, Bay L, Berumen ML, Bourne DG, Cantin N,
942   Foret S, Matz M, Miller DJ, Moya A, Putnam HM, Ravasi T, Van Oppen MJH, Thurber
943   RV, Vidal-Dupiol J, Voolstra CR, Watson S-A, Whitelaw E, Willis BL, and Munday PL.
944   2017. Rapid adaptive responses to climate change in corals. *Nat Clim Change* 7:627-636.
945   10.1038/nclimate3374
946 Vieira C, Thomas OP, Culioli G, Genta-Jouve G, Houlbreque F, Gaubert J, De Clerck O, and
947   Payri CE. 2016. Allelopathic interactions between the brown algal genus Lobophora
948   (Dictyotales, Phaeophyceae) and scleractinian corals. *Scientific Reports* 6:18637.
949   10.1038/srep18637
950 Weis VM. 2008. Cellular mechanisms of Cnidarian bleaching: stress causes the collapse of
951   symbiosis. *J Exp Biol* 211:3059-3066.
952 Welch BL. 1951. On the Comparison of Several Mean Values: An Alternative Approach.
953   *Biometrika* 38:330-336. 10.2307/2332579

954   Wiedenmann J, D'Angelo C, Smith EG, Hunt AN, Legiret F-E, Postle AD, and Achterberg EP.
955   2013. Nutrient enrichment can increase the susceptibility of reef corals to bleaching.
956   *Nature Climate Change* 3:160-164.
957   Winston M. 2022. Coral taxonomy and local stressors drive bleaching prevalence across the
958   Hawaiian Archipelago in 2019. *PLoS ONE* in-press:PONE-D-21-36063.
959   Wooldridge SA. 2013. Breakdown of the coral-algae symbiosis: towards formalising a linkage
960   between warm-water bleaching thresholds and the growth rate of the intracellular
961   zooxanthellae. *Biogeosciences* 10:1647-1658. 10.5194/bg-10-1647-2013
962   Wooldridge SA, and Done TJ. 2009. Improved water quality can ameliorate effects of climate
963   change on corals. *Ecological Applications* 19:1492-1499.
964

Mesocosm water temperature by treatment group and experimental phase.

Water temperature (ºC) measured from mesocosm water every 30 minutes. Mean ± SE temperature is shown by treatment group and experimental phase in addition to percentage of time tank temperature was ≥ 29Cº and ≥ 30Cº. Treatment group abbreviations: A (ambient heat and nutrients), N (ambient heat and enriched nutrients), NH (elevated heat and enriched nutrients), and H (elevated heat and ambient nutrients).

1 **Table 1.** Water temperature (ºC) measured from mesocosm water every 30 minutes. Mean ± SE temperature is shown
2 by treatment group and experimental phase in addition to percentage of time tank temperature was ≥ 29Cº and ≥ 30Cº.
3 Treatment group abbreviations: A (ambient heat and nutrients), N (ambient heat and enriched nutrients), NH (elevated
4 heat and enriched nutrients), and H (elevated heat and ambient nutrients).

Temperature (ºC)	A	N	NH	H
Acclimation	28.03 ± 0.35	28.02 ± 0.39	28.03 ± 0.39	28.01 ± 0.35
≥ 29Cº	10.2%	9.7%	9.5%	9.5%
≥ 30Cº	0.3%	0.4%	0.2%	0.3%
Heating	28.52 ± 0.51	28.48 ± 0.46	30.70 ± 0.52	30.73 ± 0.51
≥ 29Cº	26.0%	25.6%	99.8%	100.0%
≥ 30Cº	4.0%	3.8%	83.4%	87.7%

Mesocosm nutrient concentrations by treatment group and phase.

Nutrient concentrations (μM) measured from tank water every ~1 week. Above: comparisons of mean nutrient concentrations between aggregated enriched and ambient tanks (mean ± SE). Below: mean ± SE temperature by treatment group and experimental phase. Pairwise statistical comparisons of nutrient concentrations between treatment groups by phase are shown in Table S1.

1   **Table 2.** Nutrient concentrations (µM) measured from tank water every ~1 week. Above: comparisons of mean
2   nutrient concentrations between aggregated enriched and ambient tanks (mean ± SE). Below: mean ± SE temperature
3   by treatment group and experimental phase. Pairwise statistical comparisons of nutrient concentrations between
4   treatment groups by phase are shown in Table S1.

Nutrients (µM) by Treatment	Enriched	Ambient	Difference	*p*-value
PO_4^{-3}	1.05 ± 0.77	0.39 ± 0.35	0.62	**≤0.001**
$NO_2^- + NO_3^-$	0.75 ± 0.45	0.09 ± 0.05	0.67	**≤0.001**
NH_4^+	1.16 ± 0.64	0.23 ± 0.19	0.93	**≤0.001**
Nutrients (µM) by Phase				
Acclimation				
	A	H	N	NH
PO_4^{-3}	0.207 ± 0.044	0.346 ± 0.294	0.784 ± 0.500	0.759 ± 0.284
$NO_2^- + NO_3^-$	0.226 ± 0.044	0.173 ± 0.019	0.524 ± 0.150	0.402 ± 0.105
NH_4^+	0.238 ± 0.084	0.099 ± 0.021	0.550 ± 0.192	0.341 ± 0.058
Heating				
	A	H	N	NH
PO_4^{-3}	0.218 ± 0.117	0.570 ± 0.433	0.938 ± 0.484	1.213 ± 1.069
$NO_2^- + NO_3^-$	0.086 ± 0.053	0.089 ± 0.039	0.777 ± 0.435	0.721 ± 0.498
NH_4^+	0.202 ± 0.155	0.261 ± 0.219	1.181 ± 0.609	1.132 ± 0.713

Figure 1

Experimental design with sample sizes, and representative photograph of mesocosms.

Graphic nested study design (above) showing sample size of each treatment species and treatment group, with photograph of mesocosm system (below) depicting designated tanks by treatment (A = ambient heat and nutrients, N = ambient heat and enriched nutrients, NH = elevated heat and enriched nutrients, and H = elevated heat and ambient nutrient).
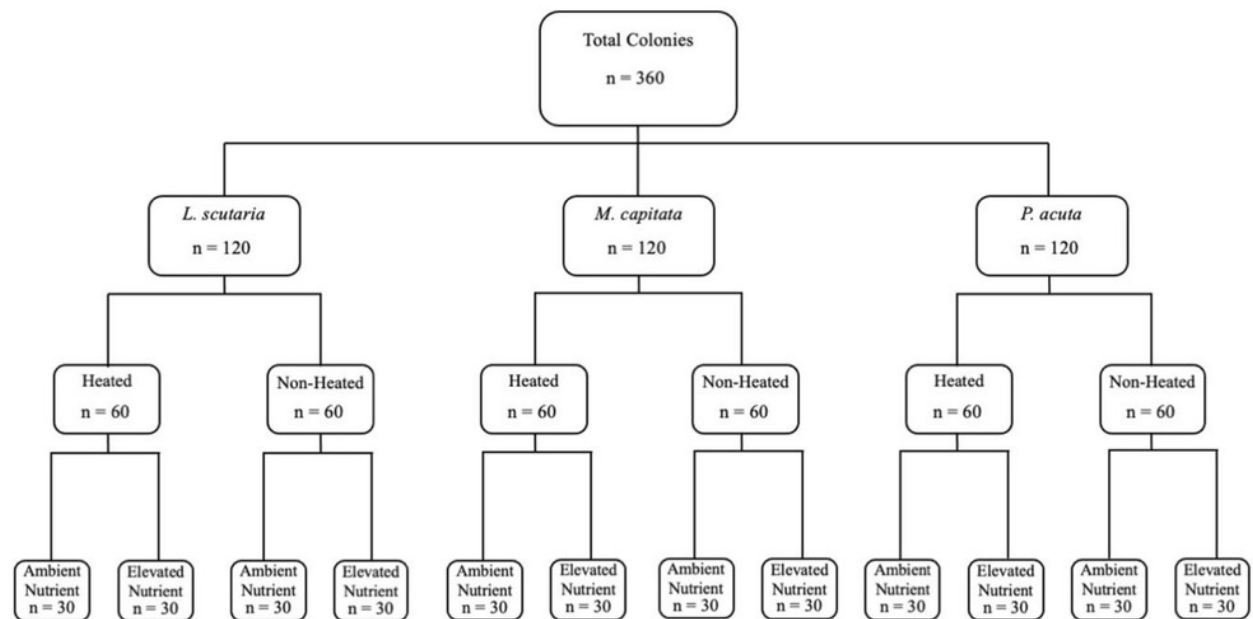
Figure 2

Timeline of study period.

Timeline of study period denoting phase periods and dates of data collection.
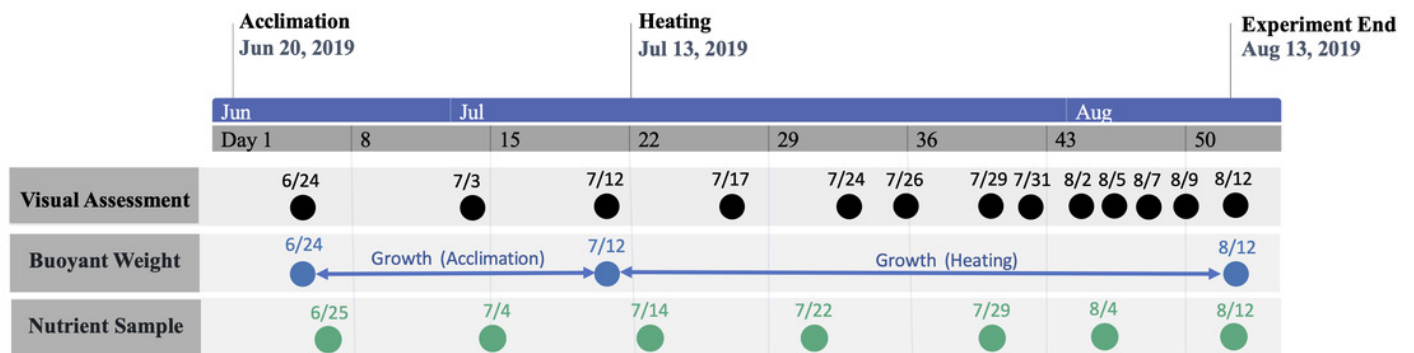
Figure 3

Aerial image of sampling location and collection area.

Aerial image of colony collection sites near Moku o Loʻe (red) and field nutrient sampling sites (yellow). Field site (South Bay and Intake Pipe) nutrient concentrations were compared with ambient mesocosm concentrations to assess uniformity between field and mesocosm conditions. Service Layer Credits: Esri, DigitalGlobe, GeoEye, Earthstar Geographics, CNES/Airbus DS, USDA, USGS, AeroGRID, IGN, and the GIS User Community.

Figure 4

Photographs of coral conditions for each study species.

Representative photographs of coral colony conditions used in visual assessments. Left to right: normal, pale, bleached, and dead. Top to bottom: *L. scutaria*, *M. capitata*, and *P. acuta.*
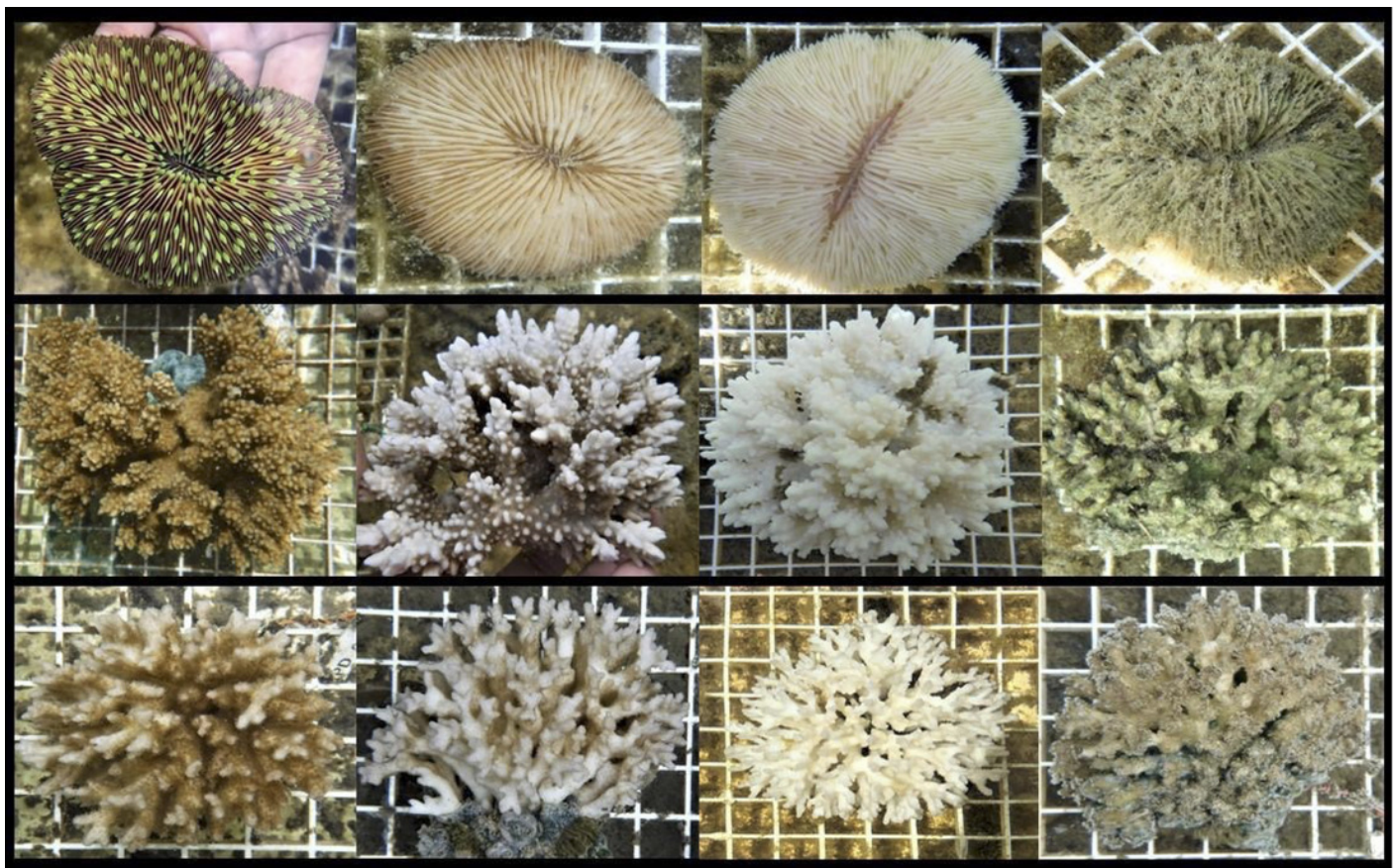
Figure 5

Partial bleaching and mortality during the heating phase.

Mean ± SE partial bleaching and mortality (%) during the heating phase for NH (black lines) and H (red lines) treatment groups shown by species. Dotted lines depict partial bleaching whereas solid lines represent partial mortality.

Lobactis scutaria

Montipora capitata

Pocillopora acuta
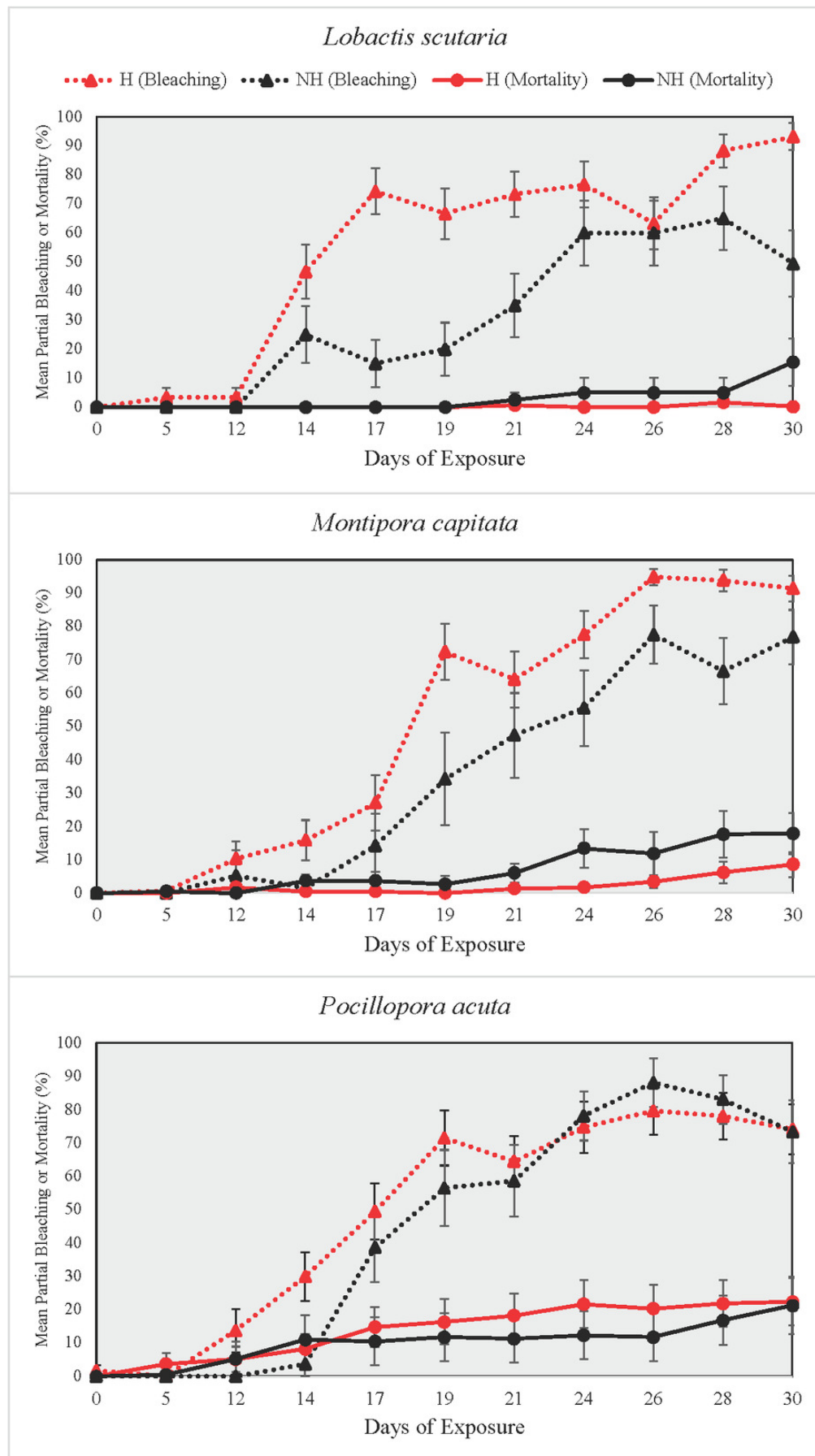
Figure 6

Calcification rate by treatment group and species.

Mean change in calcification rate (mm/day, "calcification-*d*") from the end of acclimation phase to end of heating phase by treatment and species. Pairwise comparisons of calcification-*d* between treatment groups are shown using brackets: NS = not significant, (*) = $p \leq 0.05$, and (***) = $p \leq 0.001$).
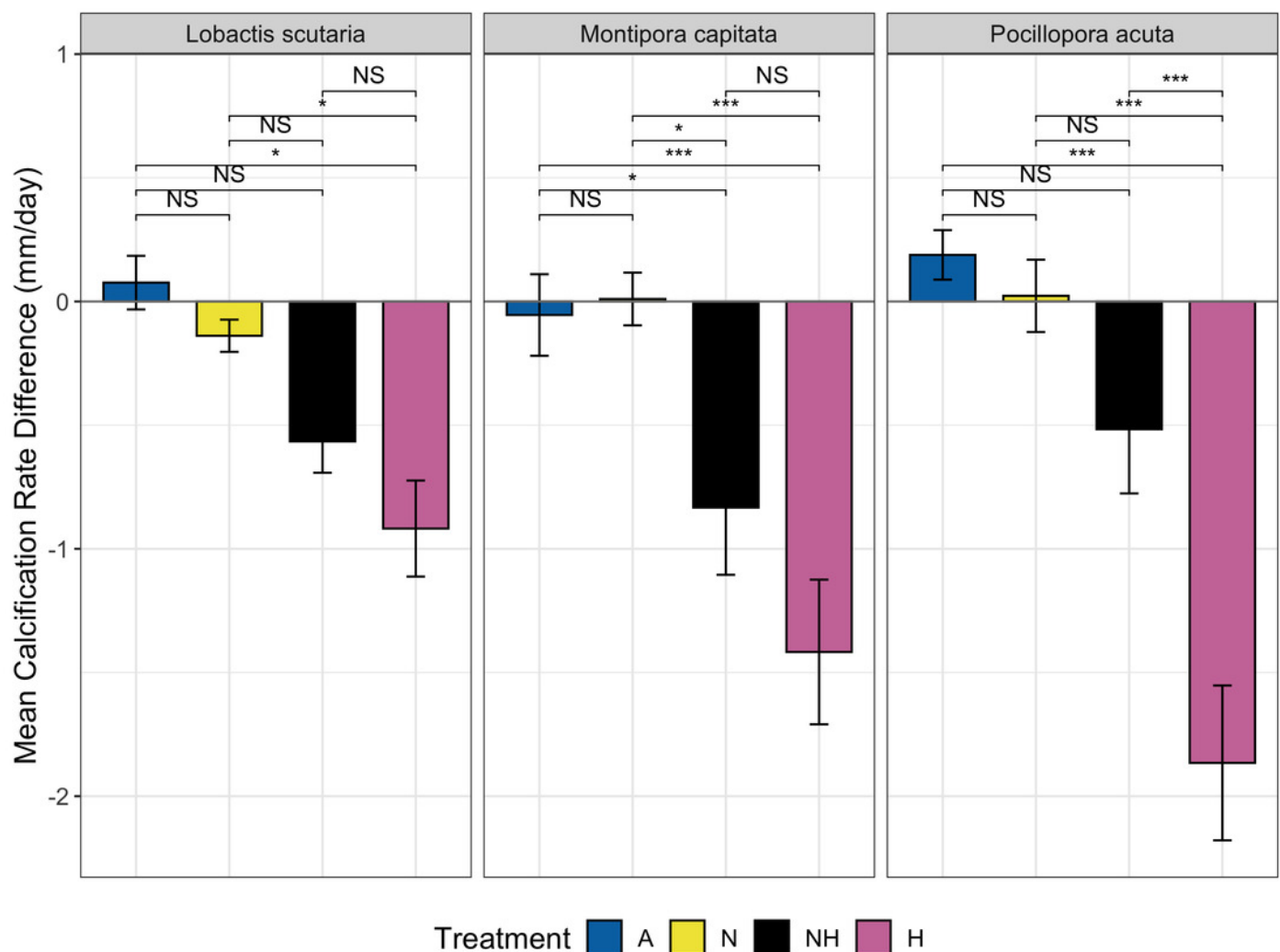
Figure 7

Visual assessment on day 12 of heating between treatment groups by species.

Percentage (%) of colonies that were either normal, pale, bleached, or dead by treatment group and species by Day 12 of the heating period.
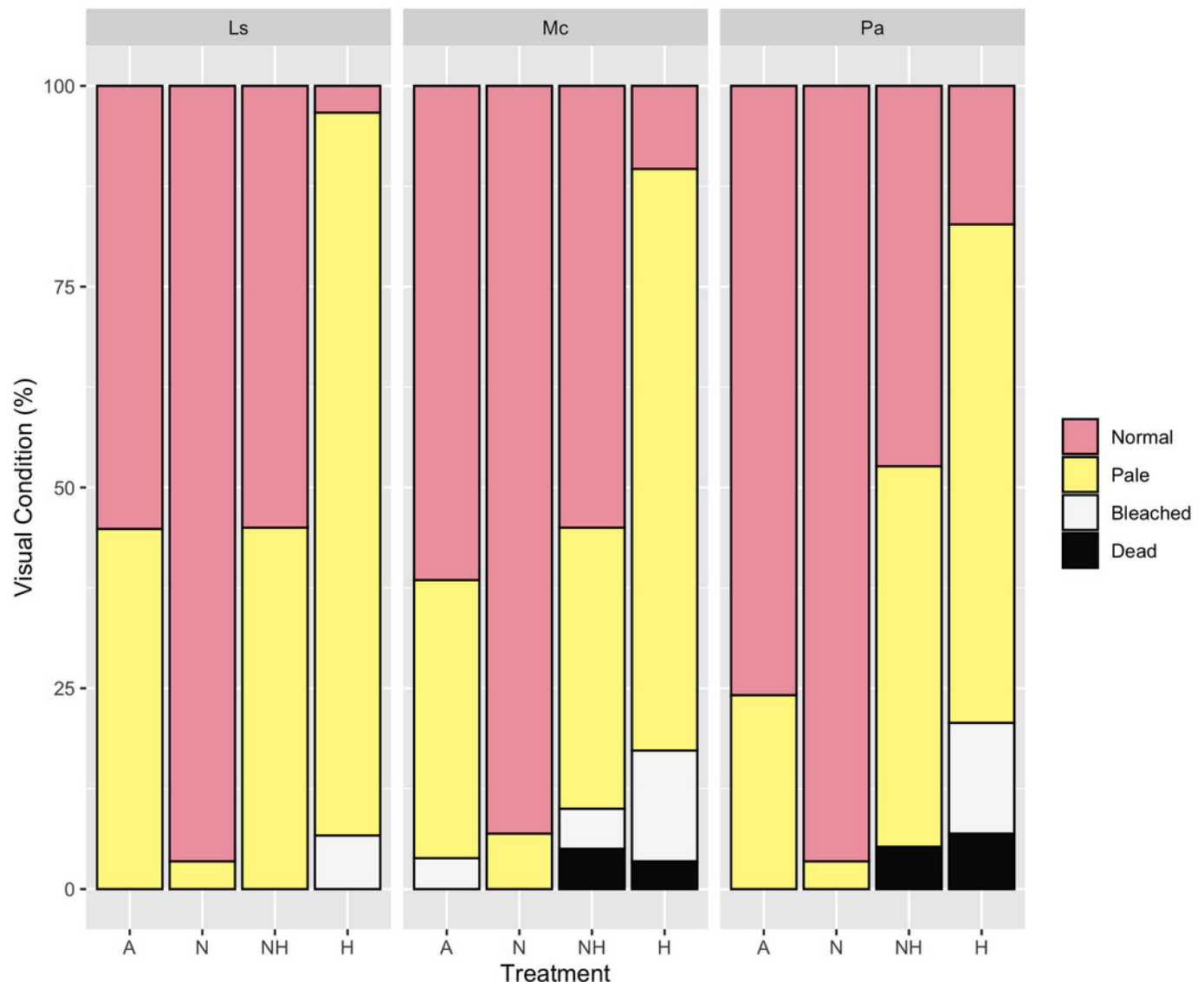
Figure 8

Multiple Correspondence Analysis (MCA) plot by treatment group on day 12.

Multiple Correspondence Analysis (MCA) plot of treatment, species, and visual assessment data from Day 12 of the heating period. Treatment group centroids are shown along with corresponding 95% CI ellipses.